Moure, M.M., Sánchez-Sáez, S., Barbero, E., & Barbero, E.J. (2014). Analysis of damage localization in composite laminates using a discrete damage model. *Composites: Part B*, 66, pp. 224-232.

DOI:10.1016/j.compositesb.2014.05.015

Analysis of damage localization in composite laminates using a discrete damage model

M.M. Moure [a], S. Sanchez-Saez [a], E. Barbero [a,*], E.J. Barbero [a,b]

[a] *Universidad Carlos III de Madrid, Spain*
[b] *West Virginia University, USA*

A B S T R A C T

Damage localization around stress raisers and material defects in laminated composites is studied using a discrete damage mechanics model augmented by a fiber damage model. The proposed formulation captures the damaging behavior of plates with initial defects and stress raisers such as holes, including damage initiation, evolution, and ultimate fracture of the specimen. It also helps explain the reduction of stress concentration factor when matrix and fiber damage develop. The state variables are the crack density and the fiber failure damage. The formulation is implemented as a material model in Abaqus applicable to laminated composite plates and shells. Material defects are simulated by inserting an initial crack density in a small region of the specimen. Stress raisers are simulated by an open hole. The predictions are shown to be insensitive to mesh density. Further, damage localizes near stress raiser and material defects, thus numerically demonstrating the objectivity of the proposed model. Qualitative and quantitative comparisons with experimental data are presented.

Keywords: Polymer–matrix composites (PMCs), Transverse cracking, Damage mechanics, Finite element analysis (FEA), Objectivity

1. Introduction

The development of models able to reproduce damage evolu tion and its effect on the stress and strain fields of a laminate is of great importance in order to reduce the number of tests neces sary for the certification of a structural element. Modeling the progressive failure of composite laminates is a complex task, due to the interaction of several failure mechanisms. This problem cannot be considered completely solved [1].

There are several methodologies to model the failure of com posite materials which have been used in the scientific literature, as *failure criteria* (usually stress based) or *continuum damage mechanics (CDM)* models. The two methods are often combined, using failure criteria to predict the onset of the damage and a CDM model to predict its evolution [2]. These methodologies have some limitations.

Failure criteria provide information about the onset of damage but not about its evolution, so that for composites that experience damage evolution prior to ultimate failure, these criteria are not sufficient. Several phenomenological criteria have been developed, many of which consider several failure mechanisms such as fiber breakage, fiber buckling, and matrix cracking, [3]. These formulations have been used for modeling brittle composites such as CFRPs subjected to different load states [4 7]. To model the loss of stiffness caused by damage, empirical coefficients are usually used to modify the elastic properties of the lamina. Several degra dation proposals appear in the literature; in some of them the elastic properties of the lamina are reduced to a fraction of the non damaged value once the failure criterion is verified [8 10].

CDM models homogenize the damage by reducing the stiffness using a second or fourth order phenomenological damage tensor by fitting the evolution of damage variables with an evolution equation. These models require parameters that are difficult to determine experimentally. Other problems of this methodology are their mesh size dependence and the difficulty to describe the local effects of the stress redistribution on the damage zone [11]. Several models employing CDM can be found in the literature [12 16].

An alternative to these methodologies is *discrete damage mechanics (DDM)* [11,17]. These models are able to predict accu rately the strain at which the first crack appears, how crack density evolves as a function of applied strain, and how stresses are redis tributed in the laminate due to the degradation of the mechanical properties of the cracked lamina.

Among the models based on this methodology, [17] has the advantage of simplicity, requiring only one state variable per lamina the crack density of the lamina to keep track of damage

* Corresponding author. Tel.: +34 916299965.
E-mail address: ebarbero@ing.uc3m.es (E. Barbero).

initiation, evolution, and strain softening, while using standard, displacement based elements in a commercial *finite element analysis (FEA)* program. This model predicts matrix cracking initiation and evolution, and calculates stress redistribution in all the laminae.

Matrix cracking appears in laminae subjected to transverse tensile load and/or inplane shear. However, [17] does not predict laminate failure because it does not include fiber failure. Fiber failure is usually brittle and can be characterized by a Weibull statistical distribution [18].

A model meant to analyze damage evolution must be able to predict damage localization. The damage of a laminate usually begins at points of stress concentration, such as material defects or stress raisers (e.g., holes, fillets, etc.). Many authors use the problem of a laminate with a hole to validate damage models due to the complex stress fields close to the hole caused by stress concentration and anisotropy of the material [11,15,19 21], but they usually study the failure load and not how the presence of the hole affects the onset and evolution of damage.

Due to the complexity of the phenomenon, damage evolution in laminates is usually studied using numerical models [21]. A critical point of the numerical modeling is the dependence of the results on mesh refinement (mesh density) [22]. Usually, successive mesh refinement is necessary [18]. In CDM models, usually a characteristic length is used to alleviate mesh dependency [15,23]. Therefore, it would be of great interest to have mesh independent numerical models that do not require the use of a characteristic length.

In this work, the applicability of the DDM methodology [17] is extended to include fiber failure by incorporating a simple fiber damage model requiring just one additional material property. Then, the proposed formulation is shown to predict damage localization and ultimate fracture results that are mesh independent and in good agreement with qualitative and quantitative experimental data for open hole tension [19].

2. Discrete damage model

To study damage localization, the discrete damage model [17] is selected. A simple fiber damage model is added to estimate the transition to fiber failure that precedes ultimate fracture of the laminates studied, that is, laminates with a minor defect and with a stress raiser, specifically with an open hole under tension. The combined formulation is then implemented as a user general section (UGENS) in Abaqus [23]. The resulting implementation is applicable to plates and shells made of symmetric laminates under general loads.

2.1. Matrix cracking

Matrix cracking results in a set of parallel cracks, which can be represented by the crack density λ in each lamina. The crack density is defined as the inverse of the distance between two adjacent cracks (number of cracks per unit length, Fig. 1). The model is formulated on a *representative volume element (RVE)*, defined as the volume enclosed by the mid surface and the top surface of the laminate t, the surface between two consecutive cracks $2l$, and a unit length parallel to the cracks. The cracks occupy the entire thickness of the lamina, since all cracks are parallel to the fiber direction and practical designs avoid thick laminae. A unit length is chosen because it is assumed that the crack propagates along the fiber direction a distance much larger than the ply thickness. In coupons under tensile load, cracks propagate from one edge to the other of the specimen (about 25 mm). Therefore, and to afford an analytical solution, the state of damage on neighboring elements along the fiber direction is not considered in the solution. The accuracy of such assumption can be assessed only indirectly by the quality of measurable macroscopic response such as the failure load in Table 2.

Since the objective is to calculate the laminate stiffness reduction due to cracks, it suffices to work with the average thickness of the variables. Moreover, the model assumes a linear variation of interlaminar shear stress in the z direction on each lamina [17]. Therefore, both the constitutive equations and the equilibrium equations can be written in terms of the average variables. Then, the reduction of stiffness in each lamina can be calculated as a function of the crack density using these assumptions.

The model uses an uncoupled activation function [24, (1)], which is defined as a function of the strain energy release rate for modes I and II. This activation function works both as *initiation*and *damage evolution*criteria. Note that for 0/90 laminates as the ones used in this paper, the ERR mode II is zero (G_{II} 0), so the critical ERR G_{IIc} is not involved in the calculations.

This model has been validated experimentally for the same material used in this work with several stacking sequences [17,25]. The validation variable was the stiffness of the laminate and its variation with the crack density. However, [17,25] did not consider defects, stress raisers, or fiber damage.

2.2. Fiber failure

Fiber failure onset is estimated by the *maximum stress criterion (MSC)*, which can be written in the customary form $g \leqslant 0$, as follows

$$g \quad \left\langle \frac{\sigma_1}{F_{1t}} \right\rangle + \left\langle \quad \frac{\sigma_1}{F_{1c}} \right\rangle \leqslant 0 \tag{1}$$

where $g \leqslant 0$ represents the undamaging domain, F_{1t}, F_{1c} are the longitudinal tensile and compressive strength of the unidirectional lamina, and $\langle \sigma_1 \rangle \quad (\sigma_1 + |\sigma_1|)/2$. The equal sign is retained so that the *return mapping algorithm (RMA)* can be made to converge to $g \quad 0$.

Use of a failure criterion like this in nonlinear analysis is not advisable because it is strongly mesh dependent. The elastic energy stored in the volume associated to the Gauss point where the criterion is satisfied is suddenly released. This volume is proportional to the size of the element, which introduces strong mesh dependency. Without regularization, the sudden change of stiffness makes it very difficult to converge to an equilibrium solution. Therefore, a regularized degradation model is necessary.

The stochastic fiber strength is represented by a Weibull distribution [18]. When combined with a shear lag model, the amount of damage, $0 < D_{1t} < 1$, in the form of fiber breaks can be calculated as [26,27]

$$D_{1t} \quad 1 \quad exp\left[\frac{1}{m\ e}\left(\frac{\tilde{\sigma}_1}{F_{1t}}\right)^m\right] \tag{2}$$

where m is the Weibull modulus, e is the basis of natural log, and the effective stress σ_1 is calculated in term of the longitudinal stress as

$$\tilde{\sigma}_1 \quad \frac{\langle \sigma_1 \rangle}{(1 \quad D_{1t})} \tag{3}$$

where $\langle \sigma_1 \rangle$ is used to assure that only tensile stress is used in the calculation. To prevent recalculation of damage during unloading, the damage is updated only if the effective stress exceeds the hardening threshold g_{1t}, which is a state variable. In other words, the undamaging domain is

$$g \quad \tilde{\sigma}_1 \quad g_{1t} \leqslant 0 \tag{4}$$

When $g > 0$, the damage is updated with Eqs. (2) and (3) and the threshold is updated to $g_{1t} \quad \langle \sigma_1 \rangle$, where $\langle x \rangle$ is the McAuley opera

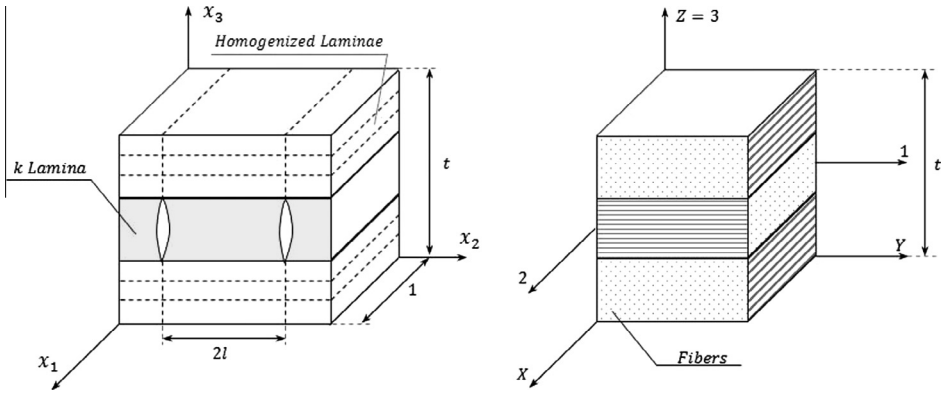

Fig. 1. Representative volume element (RVE) and coordinate system.

tor that returns only the positive part of the argument; that is, returns x if $x > 0$ and 0 if $x \leqslant 0$. Although the updating of g_{1t} repre sents hardening in effective stress space, nominal (Cauchy) stress softening can be seen by virtue of Eq. (3), i.e.,

$$\sigma_1 \quad (1 \quad D_{1t})\tilde{\sigma}_1 \tag{5}$$

Longitudinal tensile failure is brittle and, under load control, failure occurs suddenly with little accumulated damage. Also, localization results in rapid failure even when the boundary is under displacement control.

Eq. (2) provides a mechanistic regularization model that, while helping achieve numerical convergence of the structural analysis software, assures that the peak of the longitudinal stress strain curve coincides with F_{1t}. The only material properties needed are the lamina longitudinal tensile strength F_{1t} and the Weibull modulus m of the fibers. When experimental data for the Weibull modulus is not available, m can be interpreted as a numerical regularization parameter, with the advantage that experimental values of m for similar materials can be used to realistically bracket the values used. For example, a compilation of experimental values of Weibull modulus for a broad variety of composite materials is available in [28, Tables 2.3 2.4]. To assess the influence of the Weibull modulus (m) on the results of model, two values are used (m = 3.42, and 8.9). These are extreme values from a variety of carbon fiber composites reported in [28, Tables 2.3 2.4]. Analysis are made for a [0/908/0/908/0] Fiberite/HyE 9082Af laminate sub jected to tensile load with a 1.25 mm radius hole. No significant differences are observed in the results.

3. Problem description

A square plate of $a \times b$ 25×25 mm^2 made from a glass/viny lester laminate (Fiberite/HyE 9082Af) was studied. The stacking sequence selected is $[0/90_8/0/90_8/0]$. The mechanical properties of the materials are shown in Table 1, taken from the literature.

In this work, the model is implemented in Abaqus/Standard by programming a user subroutine UGENS [23]. Due to symmetry conditions, only a quarter of the plate is modeled with its corre sponding boundary conditions, and a horizontal displacement is applied to simulate a uniaxial tensile load. The meshing is carried out using quadratic rectangular elements (S8R) and triangular ele ments (STR165).

Two problems are analyzed, as shown in Fig. 2. First a laminate with a defect in the center of the plate, and second a laminate with a hole located also at the center of the plate. These cases are used to study the *objectivity* of the model, i.e., sensitivity of the result to mesh refinement and localization of damage near the initial dam age and the stress raiser.

Table 1
Mechanical properties of Fiberite/HyE 9082 Af.

Property	Units	Value
Critical energy release rate, mode I, G_{IC}	(kJ/m^2)	0.254 [24]
Critical energy release rate, mode II, G_{IIC}	(kJ/m^2)	0.292[a]
Tensile strength in the fiber direction F_{1t}	(MPa)	1020[b]
Compressive strength in the fiber direction F_{1c}	(MPa)	620[b]
Tensile strength in transversal direction F_{2t}	(MPa)	40[b]
Compressive strength in transversal direction F_{2c}	(MPa)	140[b]
Shear strength F_6	(MPa)	60[b]
Transition thickness t_t	(mm)	0.6[c]
Weibull modulus m	–	8.9[d]
Young modulus in the fiber direction E_1	(MPa)	44,700 [24]
Young modulus in transversal direction E_2	(MPa)	12,700 [24]
In-plane shear modulus G_{12}	(MPa)	5800 [24]
In-plane Poisson's ratio v_{12}	–	0.297 [24]
Out-of-plane Poisson's ratio v_{23}	–	0.41 [17]
Lamina thickness t_k	(mm)	0.144 [24]

[a] Estimated [28, (7.39)].
[b] [28, Table 1.3, col. 1].
[c] [28, §7.2.1].
[d] [28, Table 2.3].

4. Results

4.1. Mesh dependence

For both problems, plate with a defect and plate with stress rai ser, three discretizations are used to analyze global response and damage evolution as a function of mesh density. The plate is square and symmetry conditions are used to reduce the model to a quarter plate (Fig. 3). The plate is subjected to a uniform applied displace ment at x $a/2$, thus simulating a uniform applied strain.

The plate with 1.25 mm radius hole is discretized as seen in Fig. 3 with a combination of S4R and STR165 elements, using 72, 299, and 1498 elements, respectively. For the plate with a defect, the three discretizations are uniform, using 144, 625, and 2500 S4R elements, respectively.

A defect is simulated by inserting an initial crack density (0.09 mm ^{1}) at the center of the plate (i.e., at the corner of the dis cretization with symmetry boundary conditions). The rest of the plate is assigned a low value of crack density (0.02 mm ^{1}) to seed the model for possible damage initiation. The plate with a hole has no defect; only uniform seed damage is used.

The lack of influence of mesh density on the global response of the plate is corroborated by the load displacement curves for both problems studied. As it is shown in Fig. 4, the difference between the results from the three discretizations is negligible for both problems.

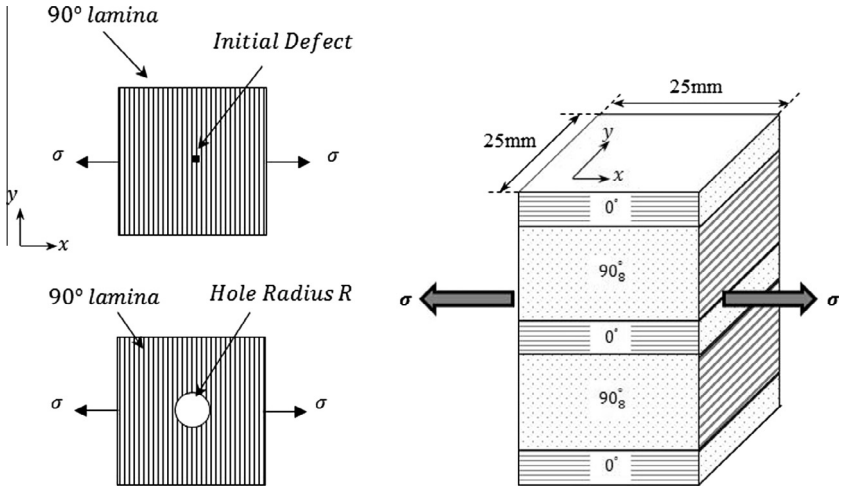

Fig. 2. Two problems are analyzed: a plate with a defect (top left) and a plate with a hole (bottom left).

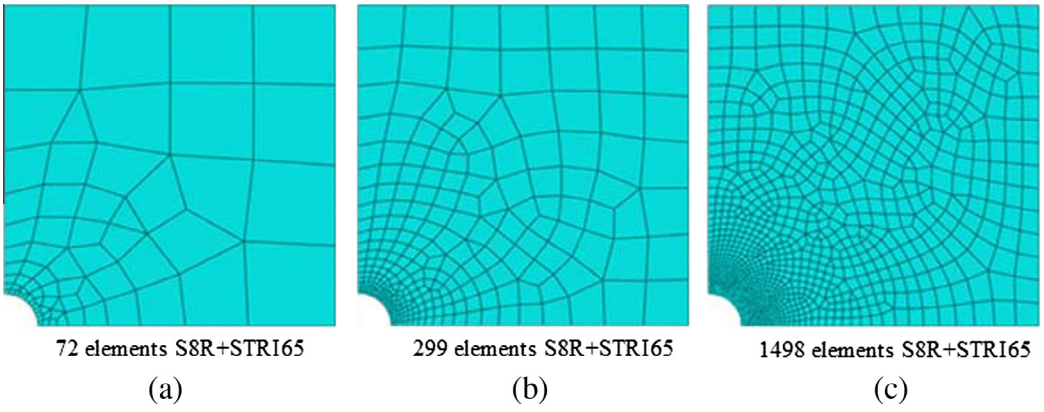

Fig. 3. Discretization used to study the plate with a hole.

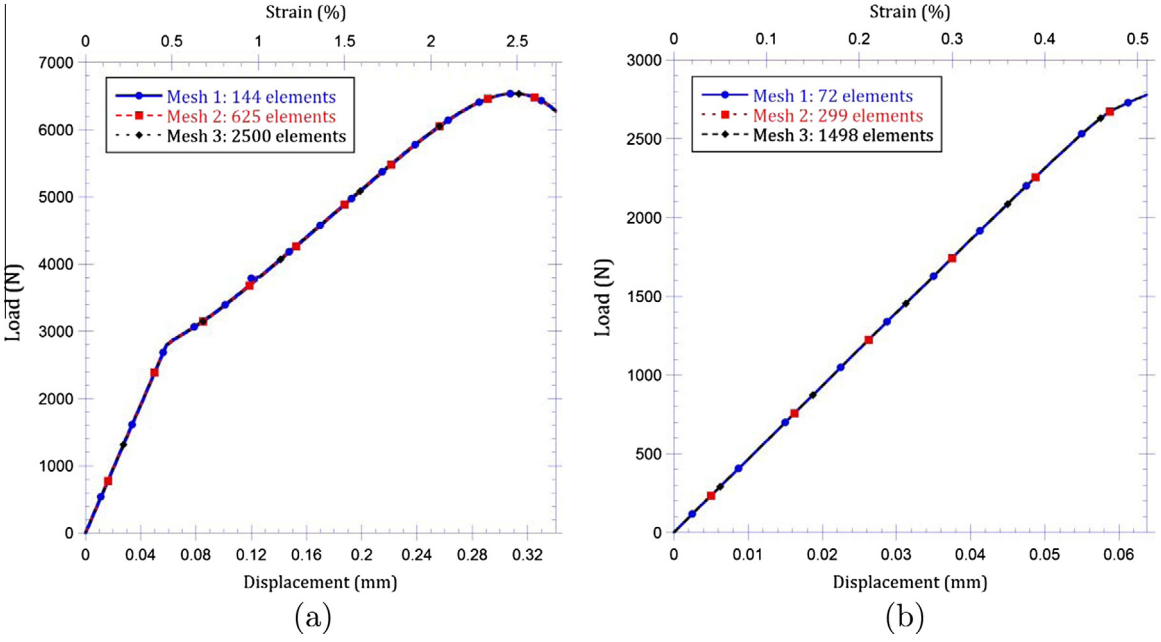

Fig. 4. Load–displacement response: (a) plate with defect, and (b) plate with a hole.

Also, the influence of mesh refinement was analyzed in relation to crack density evolution. The evolution of crack density in the element with initial damage is shown in Fig. 5(a). The evolution of crack density in the element at the edge of the hole ($x \quad 0, y \quad r$) is shown in Fig. 5(b). It can be seen that the differences are negligible.

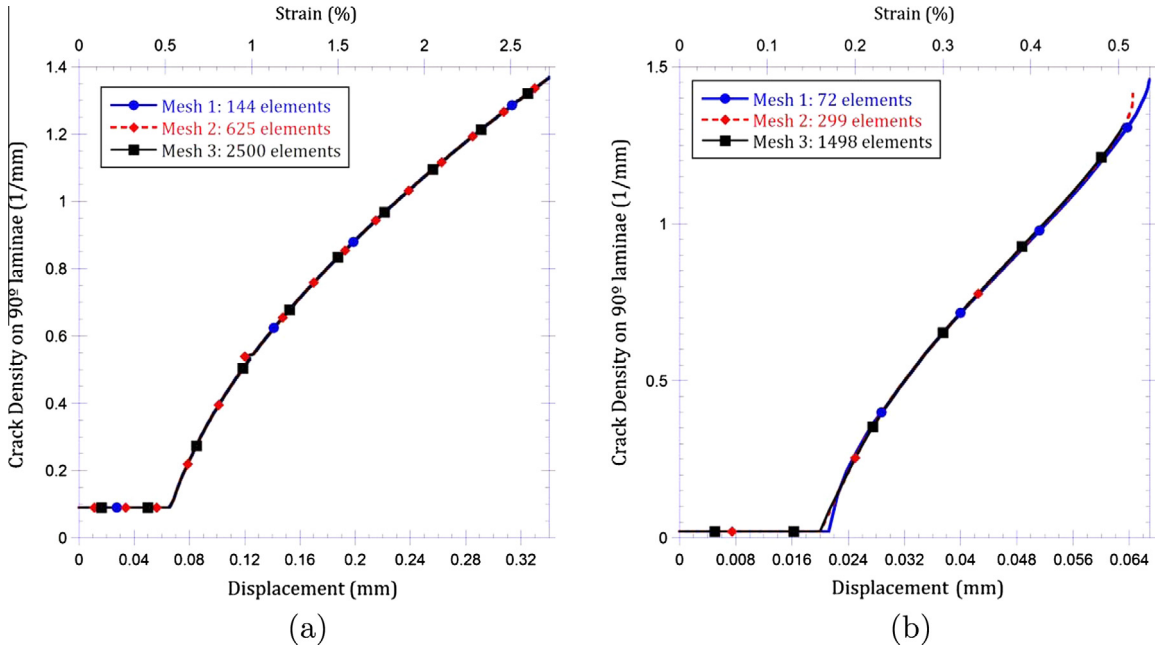

Fig. 5. Crack density evolution: (a) plate with defect, and (b) plate with a hole.

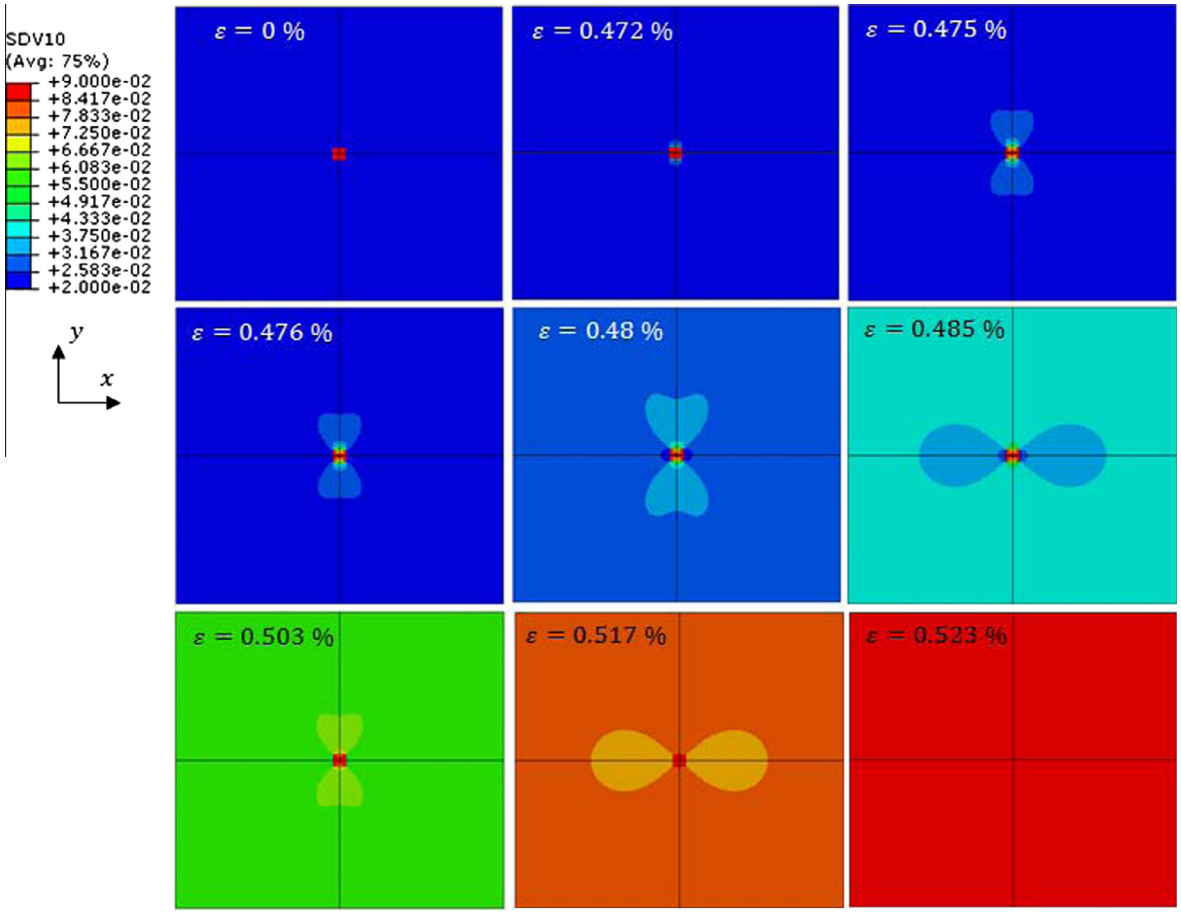

Fig. 6. Crack density in the 90-deg center cluster for applied strain up to 0.523%.

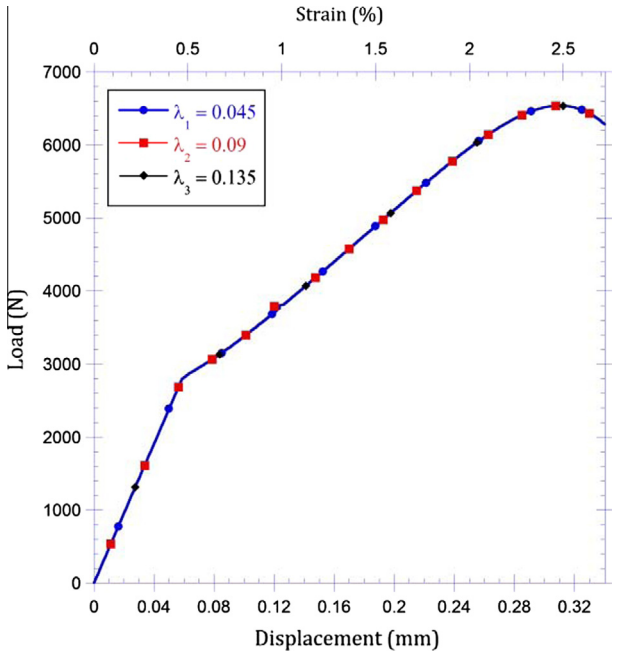

Fig. 7. Force–displacement response for various values of defect crack density.

Similar mesh independence can be corroborated at all locations on the plate. From these observations, it can be concluded that the results provided by the proposed formulation are mesh independent.

4.2. Damage localization

4.2.1. Plate with defect

For a specimen with a defect, the load displacement curve in Fig. 4(a) is linear up to 0.47% applied strain, at which point damage propagates quickly to the whole plate. It can be seen how the resid ual modulus of the laminate drops significantly at this critical point. After that, the load displacement curve is almost linear until 2.17% applied strain, where fiber damage begins.

Damage localization is shown in Fig. 6 for a plate with a defect, showing contour plots of crack density in the 90 deg center cluster of the laminate. Damage propagates outward from the defect, perpendicularly to the load direction, and displaying a peanut shape. Crack density in the load direction is always, in every image, lower than in the rest of the plate because the area near the defect is protected in the load direction by the stress reduction caused by the defect. In the last image, at 0.523% strain, matrix damage has propagated to the entire plate.

The magnitude of crack density used to simulate the defect has no significant bearing on the results. Besides 0.09 mm $^{-1}$, two other values are used to see if they affect the results: 0.045 mm $^{-1}$, and 0.135 mm $^{-1}$, while the seed crack density in the rest of the plate is kept at the same value, 0.02 mm $^{-1}$.

A delay in the onset of crack density growth occurred when the initial value applied to the central element of the laminate was increased, continuing later on the same curve in all cases. Therefore, it can be concluded that the value of the initial crack density influences only the initial levels of applied strain but has no effect on the subsequent evolution of this parameter.

The load displacement responses are identical, irrespective of the value of crack density used to simulate the defect as long as the value is higher than the seed damage used in the rest of the plate (Fig. 7). Since load displacement reflects correct stress redis tribution and accumulated damage, all derived predictions, such as ultimate strength, will be also insensitive to the particular value of damage used for representing a defect.

4.2.2. Plate with a hole

The study of damage localization for a plate with a hole is described in this section, analyzing two hole radii: 1.25 and 4.17 mm. Linear load displacement is observed in Fig. 4(b), almost up to the ultimate load. Matrix damage starts at the edge of the hole at 0.16% applied strain (Fig. 5b), but it does not affect the lam inate moduli because the damage is localized near the edge of the hole. Only when matrix damage extends over the entire plate, at about 0.49% strain, it is possible to observe a reduction in modulus in Fig. 4(b). Soon after that, fiber damage begins to take place, which quickly leads to laminate failure. Due to the stress concen tration caused by the hole, damage localizes near the edge of the hole rather than suddenly propagating to the whole plate as in the case of the plate with a defect (described in Section 4.2.1). Therefore, the reduction of laminate modulus is small for a plate with a hole.

Prediction of ultimate strength is reported in Table 2 comparing predicted values of ultimate laminate load and experimental

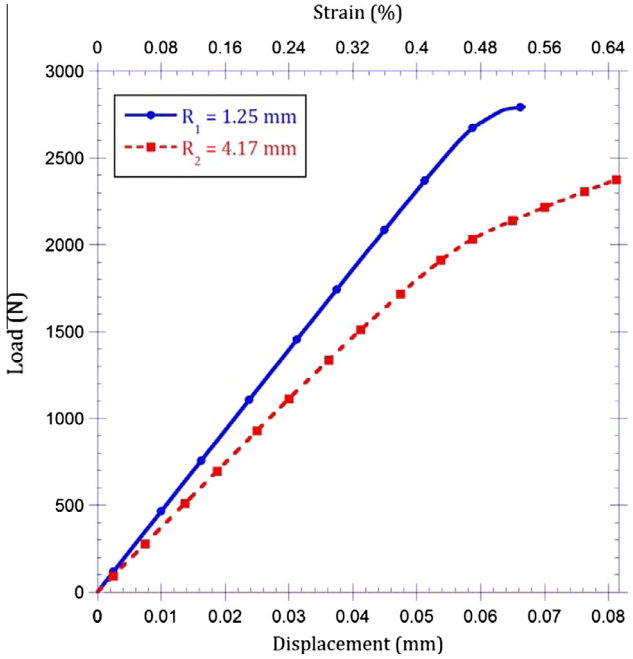

Fig. 8. Load–displacement (bottom axis) and Load–strain (top axis) for 2 hole radii: 1.25 and 4.17 mm.

Table 2
Ultimate laminate strength in MPa for $[0/\pm 45/90_7]_S$ T300/1034-C plates of width W (mm) with a hole of diameter $2R$ (mm). DDM values (in MPa) are predicted with the present model. % Error with experimental data as reference. G_{Ic} 0.228 KJ/m^2, G_{IIc} 0.455 KJ/m^2.

2R	W	2R/W	Experimental [19]	Tan [19]	Chang [34]	DDM	% Error
3.18	15.24	0.209	134.5	172.4	110.32	133	−1.1
6.35	25.4	0.25	160	158.6	103.4	142	−11.2
6.35	38.1	0.167	158.6	186.2	124.1	140	−11.7

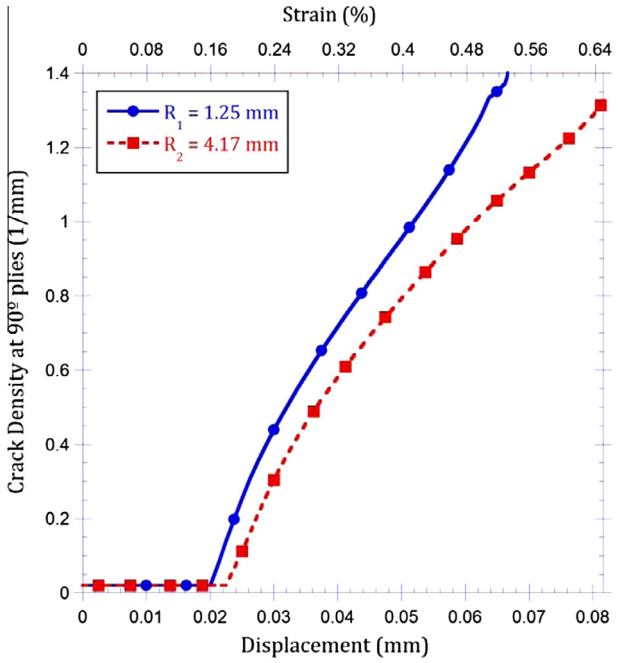

Fig. 9. Crack density at the edge of the hole.

values for $[0/\pm 45/90_7]_S$ T300/1034 C [19,29]. The error is between 1.1% and 11.7% (conservative).

The load displacementcurve for both radii studied, 1.25 and 4.17 mm, are shown in Fig. 8. The larger hole yields a laminate with lower stiffness and, due to the lower cross section, lower failure load [30]. Also, nonlinear behavior appears for a slightly lower strain 0.45% for 4.17 mm hole radius than 0.49% for 1.25 mm hole radius.

Crack density evolution on 90 deg laminae is found for both hole radii at points near the edge of the hole (Fig. 9) and near the edge of the plate (Fig. 10), where the edge effects are impor tant. Damage starts at a lower strain for a small hole. At the edge

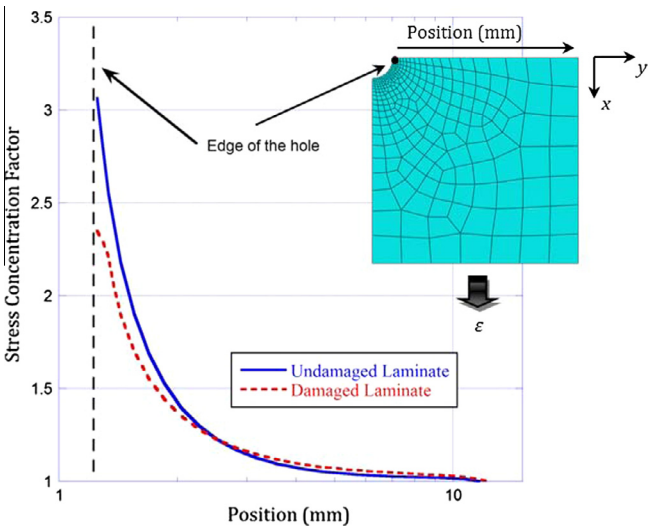

Fig. 11. SCF vs. distance from the center of the hole. Radius = 1.25 mm.

of the hole damage onset occurs at 0.16% and 0.19% for 1.25 and 4.17 mm holes, respectively. At the edge of the plate, damage onset occurs at 0.48% and 0.61%, respectively. The plate with smaller hole is stiffer, so it experiences higher stress for the same applied strain; thus, it damages earlier.

The presence of a hole causes a stress concentration at the edge of the hole (Fig. 11). The SCF depends on the laminate stacking sequence and the hole radius [31,32]. When matrix damage appears, the SCF diminishes from 3.06 for an undamaged laminate to 2.35 for a fully damaged laminate. This is in qualitative agree ment with [32].

Variation of SCF at the edge of the hole is shown in Fig. 12 as a function of applied strain. SCF starts to decrease at point 2, coincident with the onset of damage. It continues to decrease from point 2 to a minimum at point 3. When the crack density on the elements located on the edge of the hole reaches a value

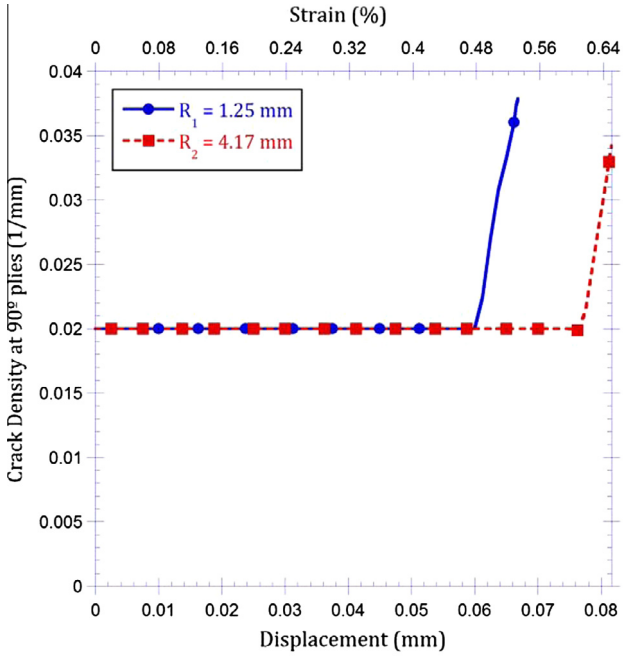

Fig. 10. Crack density at the edge of the plate.

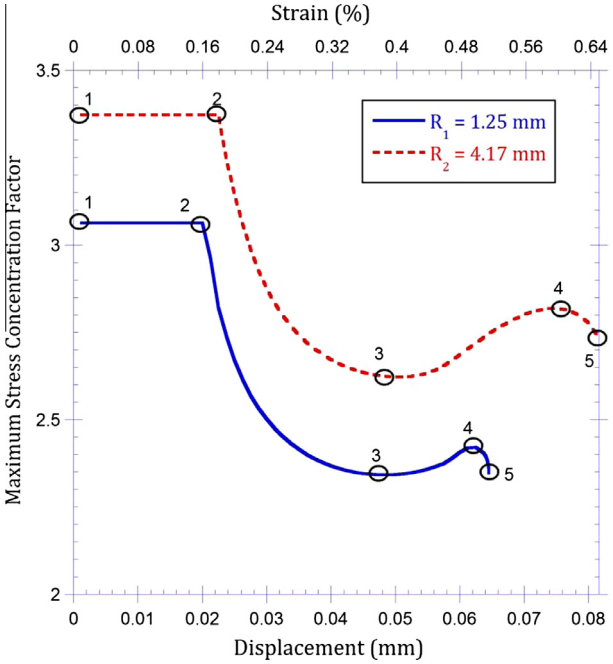

Fig. 12. SCF at the edge of the hole.

approximately equal to the inverse of the thickness of the 90 deg cluster (0.867 mm ^{1}), the SCF reaches a minimum value at the edge of the hole (point 3). When the level of damage in the 90 deg laminae is high, its loading capacity is reduced, so that most of the load is borne by 0 deg laminae. Then, the elements near the hole behave similarly to a unidirectional laminate for which the 90 deg laminae have been discounted. Therefore, the SCF at the edge of the hole slightly increases (between points 3 and 4). When the load is close to causing failure, damage to the fibers causes the SCF to decrease again (point 5).

In Fig. 12, the calculated SCF for an undamaged laminate is lar ger for the plate with larger hole radius (SCF = 3.37 for R = 4.17 mm

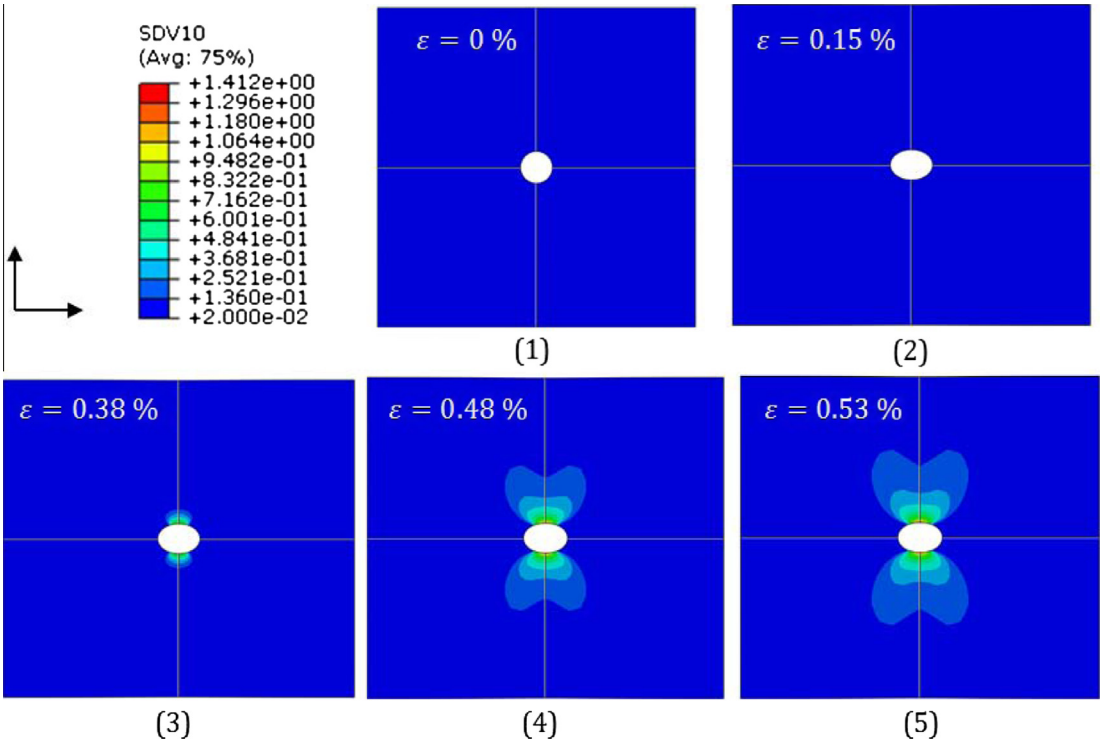

Fig. 13. Crack density corresponding to points in Fig. 12 for hole diameter 1.25 mm.

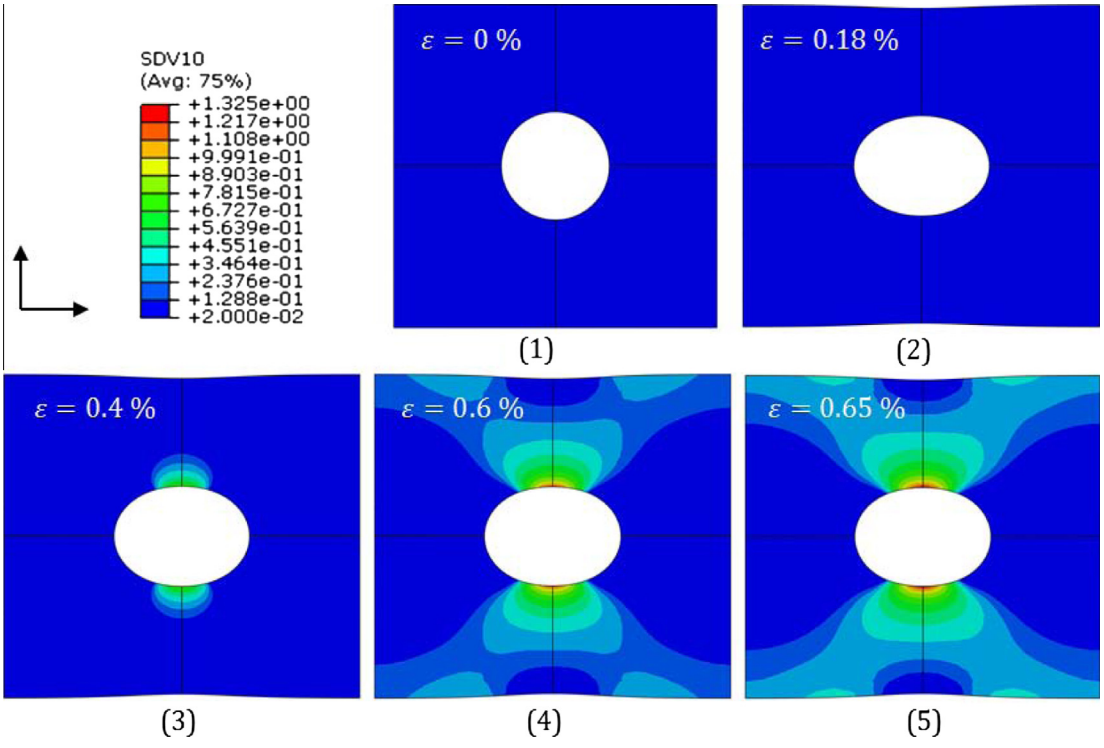

Fig. 14. Crack density corresponding to points in Fig. 12 for hole diameter 4.17 mm.

vs. SCF = 3.06 for R = 1.25 mm). These values are consistent with the results obtained applying the model of Whitney and Nuismer [31], [28, Eqs. (7.67 68), p. 260], which yields SCF = 3.5 for R = 4.17 mm and SCF = 3.02 for R = 1.25 mm.

For both hole radii, the model localizes the damage near the hole. Crack density evolution for both radii is presented in Figs. 13 and 14, for the applied strain levels shown in Fig. 12, point 1 through 5. The area with the higher crack density corresponds to the elements near the edge of the hole in the perpendicular direc tion to the load application. Damage decreases stiffness and causes a redistribution of stresses to the sides of the plate. In both cases damage propagating perpendicular to the load application has a peanut shape, with the edge perpendicular to the applied load. For the applied strain level that causes the greatest reduction of SCF (point 3 in Fig. 12), damage is highly focused on points near the edge of the hole for both diameters (Figs. 13(3) and 14(3)). As strain increases, damage extends to a larger area. The plates with smaller and larger radii differ in that for the larger hole radius, crack density reaches the edge of the plate before ultimate fracture, but for the smaller radius it does not [33].

5. Conclusions

The load displacement response and crack density evolution of various laminates featuring initial damage or stress raisers is completely insensitive to mesh density (Figs. 4 and 5).

Localization is strong (Figs. 6, 13, 14) and it has a significant effect on the SCF of stress raiser cases (Figs. 11 and 12).

The global effect of a point defect is independent of the crack density chosen to simulate the defect (Fig. 7), which is important because it frees the analyst from having to make such choice.

The SCF at the edge of the hole decreases quickly as damage develops in that zone (Fig. 12). Once damage is fully developed, the laminate behaves like a unidirectional laminate, similarly to having discounted the 90 deg laminae. Then, SCF decreases again as a result of fiber damage, but that quickly results in ultimate fracture of the laminate (Fig. 12).

The correlation between notched strength predicted by the pres ent model and experimental results is comparable to those achieved with other methodologies, and even better in some cases (Table 2). Therefore, the model may be considered as being validated.

The combination of DDM to predict matrix cracking and a Weibull controlled fiber damage model results in a formulation with the minimum number of additional material properties (namely intralaminar fracture toughness and Weibull modulus), that is able to predict damage onset, evolution, and laminate ultimate strength. The formulation works well, independently of mesh refinement, when incorporated into a classical, displace ment based finite element formulation. Implementation as a UGENS in Abaqus allows for the analysis of laminated plates and shells as long as the laminate stacking sequence is symmetric.

References

[1] Yang D, Yea J, Tan Y, Sheng Y. Modeling progressive delamination of laminated composites by discrete element method. Comput Mater Sci 2011;50(3): 858–64.

[2] Liu P, Xing L, Zheng J. Failure analysis of carbon fiber/epoxy composite cylindrical laminates using explicit finite element method. Compos Part B: Eng 2014;56:54–61.

[3] Orifici AC, Herszberg I, Thomson RS. Review of methodologies for composite material modelling incorporating failure. Compos Struct 2008;86:194–210.

[4] Santiuste C, Sanchez-Saez S, Barbero E. A comparison of progressive-failure criteria in the prediction of the dynamic bending failure of composite laminated beams. Compos Struct 2010;92(10):2406–14.

[5] Ivañez I, Santiuste C, Sanchez-Saez S. Fem analysis of dynamic flexural behavior of composite sandwich beams with foam core. Compos Struct 2010;92(9):2285–91.

[6] Gama BA, Gillespie JW. Finite element modeling of impact, damage evolution and penetration of thick-section composites 2011;38:181–97.

[7] Phadnis VA, Makhdum F, Roy A, Silberschmidt VV. Drilling in carbon/epoxy composites: experimental investigations and finite element implementation. Compos Part A: Appl Sci Manuf 2013;47:41–51.

[8] Luo RK, Green ER, Morrison CJ. Impact damage analysis of composite plates. Int J Impact Eng 1999;22:435–47.

[9] Camanho PP, Matthews FL. A progressive damage model for mechanically fastened joints in composite laminates. J Compos Mater 1999;33:2248–80.[10] Papanikos P, Tserpes KI, Pantelakis SP. Modelling of fatigue damage progression and life of CFRP laminates. Fatigue Fract Eng Mater Struct 2003;26:37–47.

[11] Swindeman MJ, Iarve EV, Brockman RA, Mollenhauer DH, Hallett SR. Strength prediction in open hole composite laminates by using discrete damage modeling. AIAA J 2013;51(4):936–45.

[12] Ladeveze P, Ledantec E. Damage modeling of the elementary ply for laminated composites. Compos Sci Technol 1992;43(3):257–67.

[13] Barbero EJ, DeVivo L. Constitutive model for elastic damage in fiber-reinforced PMC laminae. Int J Damage Mech 2001;10(1):73–93.

[14] Zou Z, Reid SR, Li S. A continuum damage model for delaminations in laminated composites. J Mech Phys Solids 2003;51(2):333–56.

[15] Maimi P, Camanho PP, Mayugo JA, Dávila CG. A continuum damage model for composite laminates: part i – constitutive model. Mech Mater 2007;39(10):897–908.

[16] Liu PF, Zheng JY. Progressive failure analysis of carbon fiber/epoxy composite laminates using continuum damage mechanics. Mater Sci Eng: A 2008;485(12):711–7.

[17] Barbero EJ, Cortes DH. A mechanistic model for transverse damage initiation, evolution, and stiffness reduction in laminated composites. Composites Part B 2010;41:124–32.

[18] Chen BY, Tay TE, Baiz PM, Pinho ST. Numerical analysis of size effects on open-hole tensile composite laminates. Compos Part A: Appl Sci Manuf 2013;47:52–62.

[19] Tan SC. A progressive failure model for composite laminates containing openings. J Compos Mater 1991;25(5):556–77.

[20] Abisset E, Daghia F, Ladevz`e P. On the validation of a damage mesomodel for laminated composites by means of open-hole tensile tests on quasi-isotropic laminates. Compos Part A: Appl Sci Manuf 2011;42(10):1515–24.

[21] Kawashita LF, Bedos A, Hallett SR. Modeling mesh independent transverse cracks in laminated composites with a simplified cohesive segment method. Comput Mater Continua 2012;32(2):133–58.

[22] Oliver J. A consistent characteristic length for smeared cracking models. Int J Numer Methods Eng 1989;28(2):461–74.

[23] Simulia, Abaqus 6.11 analysis users manual and documentation; 2011.

[24] Barbero EJ, Cosso FA, Martinez X. Identification of fracture toughness for discrete damage mechanics analysis of glass-epoxy laminates. Appl Compos Mater 2013:1–18.

[25] Barbero EJ, Sgambitterra G, Adumitroaie A, Martinez X. A discrete constitutive model for transverse and shear damage of symmetric laminates with arbitrary stacking sequence. Compos Struct 2011;93:1021–30.

[26] Kelly KW, Barbero EJ. Effect of fiber damage on the longitudinal creep of a CFMMC. Int J Solids Struct 1993;30(24):3417–29.

[27] Barbero EJ, Kelly KW. Predicting high temperature ultimate strength of continuous fiber metal matrix composites. J Compos Mater 1993;27(12):1214–35.

[28] Barbero EJ. Introduction to composite materials design. 2nd ed. Philadelphia, PA: CRC Press; 2011. <http://barbero.cadec-online.com/icmd>.

[29] Maimi P, Camanho PP, Mayugo JA, Dávila CG. A continuum damage model for composite laminates: part ii – computational implementation and validation. Mech Mater 2007;39(10):909–19.

[30] Green B, Wisnom M, Hallet S. An experimental investigation into the tensile strength scaling of notched composites. Compos Part A: Appl Sci Manuf 2007;38:867–78.

[31] Whitney JM, Nuismer RJ. Stress fracture criteria for laminated composites containing stress concentrations. J Compos Mater 1974;8:253–65.

[32] Pierron F, Green B, Wisnom MR, Hallett SR. Full-field assessment of the damage process of laminated composite open-hole tensile specimens. part ii: Experimental results. Compos Part A: Appl Sci Manuf 2007;38(11):2321–32.[33] O'Higgins R, McCarthy M, McCarthy C. Comparison of open hole tension characteristics of high strength glass and carbon fibre-reinforced composite materials. Compos Sci Technol 2008;68:2770–8.

[34] Chang F-K, Chang K-Y. A progressive damage model for laminated composites containing stress concentrations. J Compos Mater 1987;21:834–55.